Mechanism of CheA Protein Kinase Activation in Receptor Signaling Complexes†

Mikhail N. Levit, Yi Liu,‡ and Jeffry B. Stock*

Department of Molecular Biology, Princeton University, Princeton, New Jersey 08544

Received December 2, 1998; Revised Manuscript Received February 19, 1999

ABSTRACT: The chemotaxis receptor for aspartate, Tar, generates responses by regulating the activity of an associated histidine kinase, CheA. Tar is composed of an extracellular sensory domain connected by a transmembrane sequence to a cytoplasmic signaling domain. The cytoplasmic domain fused to a leucine zipper dimerization domain forms soluble active ternary complexes with CheA and an adapter protein, CheW. The kinetics of kinase activity within these complexes compared to CheA alone indicate approximately a 50% decrease in the K_M for ATP and a 100-fold increase in the V_{max}. A truncated CheA construct that lacks the phosphoaccepting H-domain and the CheY/CheB-binding domain forms an activated ternary complex that is similar to the one formed by the full-length CheA protein. The V_{max} of H-domain phosphorylation by this complex is enhanced approximately 60-fold, the K_M for ATP decreased to 50%, and the K_M for H-domain decreased to 20% of the values obtained with the same CheA construct in the absence of receptor and CheW. The kinetic data support a mechanism of CheA regulation that involves perturbation of an equilibrium between an inactive form where the H-domain is loosely bound and an active form where the H-domain is tightly associated with the CheA active site and properly positioned for phosphotransfer. The data are consistent with an asymmetric mechanism of CheA activation [Levit, M., Liu, I., Surette, M. G., and Stock, J. B. (1996) *J. Biol. Chem. 271*, 32057−32063] wherein only one phosphoaccepting domain of CheA at a time can interact with an active center within a CheA dimer.

During bacterial chemotaxis, information about the chemistry of a cell's environment is received by a family of membrane receptors with extracellular sensing domains connected to cytoplasmic signaling domains (for recent reviews, see references *1*−*5*). In response to environmental signals, these chemoreceptors modulate the activity of an associated histidine protein kinase, CheA, that together with an adapter protein, CheW, forms a ternary complex with receptor signaling domains. CheA phosphorylates one of its own histidine residues, His48, and the phosphoryl group is then rapidly transferred to a soluble response regulator protein, CheY. Phospho-CheY interacts with the flagellar motor to induce a change in the direction a cell is swimming.

The best-characterized bacterial chemoreceptor is Tar. This protein mediates responses to aspartate in *Escherichia coli* and *Salmonella*. The periplasmic aspartate-binding domain of the receptor is a four-helix bundle that forms a symmetric dimer with two nonoverlapping ligand-binding sites at the dimer interface (*6*−*8*). The cytoplasmic signaling domain of Tar is also predominantly α-helical (*9*−*14*). It is composed of a highly conserved central region termed the signaling domain that binds CheW (*9*, *15*) flanked by two sequences that are predicted to form coiled-coil structures (*9*, *16*−*18*) (Figure 1A). These sequences, termed methylated helices 1 and 2, contain glutamate and glutamine residues that are subject to methyl esterification by a specific *S*-adenosylmethionine-dependent methyltransferase, CheR (*19*, *20*), and demethylation or deamidation by a specific esterase/amidase, CheB (*21*−*23*). Structural studies of the periplasmic sensing

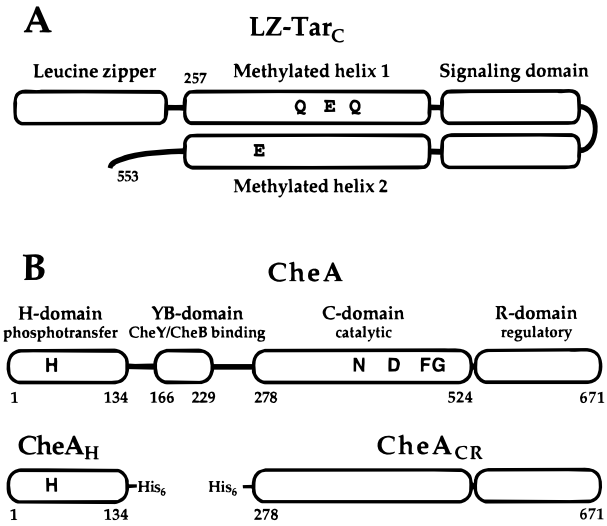

FIGURE 1: Domain organization of LZ-Tar$_c$ and CheA. (A) Schematic representation of LZ-Tar$_c$, the Tar chemoreceptor construct used in this work, where the cytoplasmic part of the receptor (residues 257−553) is fused to a leucine zipper (*9*). The representation is based on a previously proposed model for the cytoplasmic portion of Tar (*12*). Glutamates and glutamines that are subject to modification by CheR and CheB are indicated. (B) Domain structure of CheA and the CheA constructs used in this work. Approximate beginnings and ends of domains of CheA from *S. typhimurium* are shown on the basis of sequence homology to the constructs of CheA from *E. coli* whose NMR or crystal structures have been determined (see text). H, N, D, F, and G indicate the boxes of homology in the protein histidine kinases family (*35*).

† This work was supported by NIH Grant R01GM57773 to J.B.S.

* Corresponding author. Telephone: (609) 258-6111. Fax: (609) 258-6175. E-mail: jstock@princeton.edu.

‡Present address: Small Molecule Therapeutics, Inc., Monmouth Junction, NJ 08852.

10.1021/bi982839l CCC: $18.00
Published on Web 04/30/1999

domain and data on subunit cross-linking between cysteines engineered into the transmembrane or sensing domains indicate that Tar in membranes is predominantly dimeric (*24*, *25*).

CheA has been shown to exist in equilibrium between inactive monomers and active dimers (*26*). Each CheA monomer is composed of several structurally and functionally distinct domains (*27*−*29*) (Figure 1B). The phosphoaccepting His48 is located in an N-terminal four-helix bundle termed the H- or P1-domain (*30, 31*). The H-domain is followed by the YB- or P2-domain, an open-faced α/β sandwich that binds the response regulator proteins CheY and CheB (*30, 32*−*34*). Next is the catalytic C-domain that contains the highly conserved histidine kinase sequence motifs [N-, D-, F-, and G-boxes (*1, 27, 35*)] as well as the determinants for dimer formation (*1, 29*). This region functions to bind ATP and catalyze His48 phosphorylation (*28, 29, 36*). The regulatory R-domain located at the C-terminus of CheA participates in the formation of ternary complexes with CheW and receptor. The H- and YB-domains are connected to each other and to the C-domain by flexible linkers and appear to function like balls on a chain (*37, 38*). An isolated fragment of CheA corresponding to the C-domain ($CheA_C$) can phosphorylate a fragment corresponding to the H-domain ($CheA_H$) (*28, 29*).

The kinetics of CheA autophosphorylation have been extensively examined with the isolated CheA protein (*26, 29, 36, 39, 40*), but the lack of purified active CheA−CheW−receptor complexes has precluded similar detailed kinetic studies of this, physiologically more relevant, form of the enzyme. Membrane-associated enzymes are difficult to analyze kinetically because of heterogeneity and vesicular compartmentalization. To obviate these problems, aspartate receptor constructs have been generated that contain the cytoplasmic part of the receptor fused to a leucine zipper dimerization domain, LZ-Tar_C (*9, 18*). These receptor constructs form soluble ternary complexes with the kinase CheA and the adapter protein CheW. The complexes are stable for several hours and can be purified by molecular sieve chromatography (*41*). This has enabled us to study the kinetic properties of the soluble activated forms of CheA under defined conditions in vitro.

Since both Tar and CheA form dimers, it has been generally assumed that transmembrane signaling occurs within complexes formed by a dimer of receptor, a dimer of CheA, and two CheW monomers (for a review, see ref *2*). However, chemoreceptors in the bacterial membrane appear to form large arrays with CheA and CheW (*42*); studies of the structure of the ternary complexes formed with soluble fragments of the cytoplasmic domain of Tar indicate that several receptor dimers come together with CheW and CheA to form higher order structures (*41*). We have observed well-defined complexes with a stoichiometry of about 7 receptor dimers and 3 molecules of CheW per dimer of CheA. The activity of CheA in these complexes is up to 100-fold higher than that of CheA alone. To investigate the effect of glutamate modification on kinase activation, the receptor constructs were engineered in three forms: fully amidated (all Q), half-amidated (Q/E), and completely deamidated (all E). Levels of complex formation and kinase activation depended on the level of glutamate modification with complexes formed by the all-Q receptor having the highest activity.

Here we show that a fragment of CheA composed of the catalytic (C) and regulatory (R) domains, $CheA_{CR}$ (Figure 1B), can form a ternary complex with CheW and the signaling domain of Tar. The complex formed with $CheA_{CR}$ has essentially the same composition and organization as the complex formed from full-length CheA. The catalytic activity of $CheA_{CR}$ toward $CheA_H$ is 60-fold higher within this complex. This increased activity is accompanied by a significant decrease in the K_M's for both ATP and $CheA_H$. Based on these data, we propose a model wherein allosteric regulation of CheA results from a shift in equilibrium between an inactive state with the H-domain only loosely associated with the catalytic domain, and an active state with the H-domain tightly bound and properly aligned for the phosphotransfer reaction.

EXPERIMENTAL PROCEDURES

Protein Purification. The *S. typhimurium* LZ-Tar_C (*9*), CheW (*43*), CheA (*44*), CheY (*45*), and $CheA_H$ (*29*) proteins were purified as described previously. His_6-tagged *S. typhimurium* $CheA_{CR}$ was overexpressed from a derivative of pQE8 (Qiagen) that contained an insert with the corresponding *S. typhimurium cheA* fragment encoding residues 278−671 flanked by *Bam*HI and *Hin*dIII sites constructed by cloning a PCR-amplified product from the *S. typhimurium cheA* gene from pMO4 (*44*). The plasmid was transformed into *E. coli* strain M15/pREP4 (Qiagen). The final clone was confirmed by sequencing. The $CheA_{CR}$ protein was purified using the procedure described previously for purification of $CheA_C$ (*29*).

Isolation and Characterization of LZ-Tar_C−CheW−CheA Complexes. Unless indicated otherwise, to prepare active ternary complexes, a mixture of 50 μM LZ-Tar_C, 10 μM CheW, and 10 μM CheA or $CheA_{CR}$ in 25 mM Tris-HCl, 50 mM potassium glutamate, 25 mM NaCl, 5.0 mM $MgCl_2$, 10% glycerol, 5.0% DMSO, 1.0 mM dithiothreitol (DTT), pH 7.5, was incubated for 4.0 h at 30 °C as described previously (*41*). Complexes were purified by chromatography on a TSK-Gel $G5000PW_{XL}$ column (30 × 0.78 cm) with a TSK-Gel G4000PW guard column (TosoHaas), and eluted with 25 mM Tris-HCl, 50 mM potassium glutamate, 25 mM NaCl, 10% glycerol, 5.0% DMSO, pH 7.5, at a flow rate of 0.50 mL/min. The absorbance at 280 nm was monitored with a Lambda-Max Model 481 LC Spectrophotometer (Waters).

The molecular mass and hydrodynamic radius of LZ-Tar_C−CheW−CheA/$CheA_{CR}$ complexes were estimated using a miniDAWN multiple-angle laser light-scattering detector (Wyatt Technology) connected in-line with a HPLC UV detector. The light-scattering and UV absorption data were processed with ASTRA software (Wyatt Technology) to obtain absolute estimates of molecular mass (for reviews, see refs *46*, *47*). The concentration values required for molecular mass estimates were determined from UV absorption data using extinction coefficients calculated assuming 7 LZ-Tar_C:1 CheW:1 CheA/$CheA_{CR}$ stoichiometry, and corrected for the difference between the UV absorption of component proteins in the elution buffer as opposed to 6.0 M guanidine hydrochloride, 20 mM sodium phosphate, pH 6.5 (*48*). A value of 0.165 was used for the refractive index increment (dn/dc), and the solvent refractive index was estimated as 0.133.

Specimens for electron microscopic analysis negatively stained in 1% uranyl acetate were prepared as described previously (*41*).

Determination of Protein Composition of Ternary Complexes. Protein concentrations were estimated as described previously (*41*) using the BCA Protein Assay kit (Pierce) with bovine serum albumin as a standard as well as by UV absorption at 280 nm in 6 M guanidine chloride, 20 mM sodium phosphate, pH 6.5, using the following extinction coefficients in mM/cm at 280 nm calculated from the protein sequences (*48*): CheA, 14.8; $CheA_{CR}$, 10.9; $CheA_H$, 3.90; CheW, 5.18; CheY, 6.97; LZ-Tar_C, 6.97. The values obtained by the BCA Protein Assay correlated well with those obtained by absorption methods. Concentrations of individual proteins in HPLC fractions were estimated from Coomassie-stained SDS−polyacrylamide gels using a range of known amounts (0.20−2.0 μg) of the corresponding pure proteins as standards. The gels were scanned with Color OneScanner (Apple), and the images were quantified with NIH Image 1.60 software. All concentrations are expressed in terms of the indicated monomeric species.

Kinase Activity. Unless indicated otherwise, steady-state rates of ATP hydrolysis were measured in 25 mM Tris-HCl, 50 mM potassium glutamate, 25 mM NaCl, 5.0 mM $MgCl_2$, 10% glycerol, 5.0% dimethyl sulfoxide (DMSO), pH 7.5 at 23 °C, in the presence of 2.0 mM ATP and 50 μM CheY using the spectroscopic pyruvate kinase/lactate dehydrogenase-coupled assay as described previously (*41*). Molecular activities of CheA or $CheA_{CR}$ are expressed as apparent rate constants, k_{obs}, corresponding to the number of molecules of ADP produced per second per monomer of CheA or $CheA_{CR}$. Kinetic parameters (Figure 6, Tables 1 and 2) for the all-Q LZ-Tar_c−CheW−CheA complex were determined using the complex isolated from the incubation mixture by HPLC; for the all-Q LZ-Tar_c−CheW−$CheA_{CR}$ complex, aliquots of the incubation mixture were used without prior isolation of the complex because of insufficient stability of the isolated complex. Activity of the free $CheA_{CR}$ present in the incubation mixture accounted for approximately 1% of the total activity and was neglected. (We obtained identical kinetic parameters for the complex with full-length CheA using aliquots of the incubation mixture or HPLC-purified fraction of this complex.) To estimate the molecular activity, k_{obs}, of $CheA_{CR}$ within the complex with all-Q LZ-Tar_c and CheW, the rate of the reaction was measured in the presence of 100 μM $CheA_H$ and 2000 μM ATP using a freshly isolated HPLC fraction of the complex, where the concentration of $CheA_{CR}$ was estimated as described above.

RESULTS

Active Ternary Complexes Formed from the Receptor Signaling Domain, CheW, and $CheA_{CR}$. Ternary complexes between LZ-Tar_C, CheW, and $CheA_{CR}$ were formed by incubating a mixture of the three purified soluble proteins at 30 °C for 3.5−4.0 h. Complex formation was routinely assayed by following the associated increase in kinase activity (Figure 2). As with full-length CheA (*41*), a greater activation of $CheA_{CR}$ was achieved with all-Q LZ-Tar_C than with Q/E LZ-Tar_C, and no activation was observed with all-E LZ-Tar_C. Electron microscopy revealed the same kinds of structures as those obtained with full-length CheA (*41*), rod-shaped particles approximately 45 nm long and 12 nm in diameter with increased density near the middle and globular structures at the ends (Figure 3). No organized structures were observed when all-E LZ-Tar_C was incubated with $CheA_{CR}$ and CheW under the same conditions.

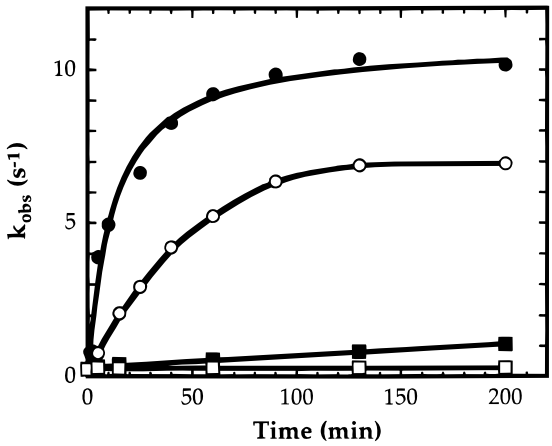

FIGURE 2: Kinase activation in the ternary complexes formed from LZ-Tar_C, CheW, and $CheA_{CR}$. Mixtures were incubated for the indicated times at 30 °C, and kinase activity was determined in the presence of 2.0 mM ATP and 50 μM CheY as described under Experimental Procedures. The kinase activity is expressed as an observed rate constant, k_{obs} [μM ATP hydrolyzed s^{-1} (μM $CheA_{total}$)$^{-1}$]. Results are presented for mixtures that contained 5.0 μM $CheA_{CR}$, 10 μM CheW, and 45 μM all-Q LZ-Tar_c (●) or Q/E LZ-Tar_c (○); a mixture of 40 μM $CheA_{CR}$, 10 μM CheW, and 45 μM Q/E LZ-Tar_c (■); and a mixture of 5.0 μM $CheA_{CR}$, 70 μM CheW, and 45 μM Q/E LZ-Tar_c (□).

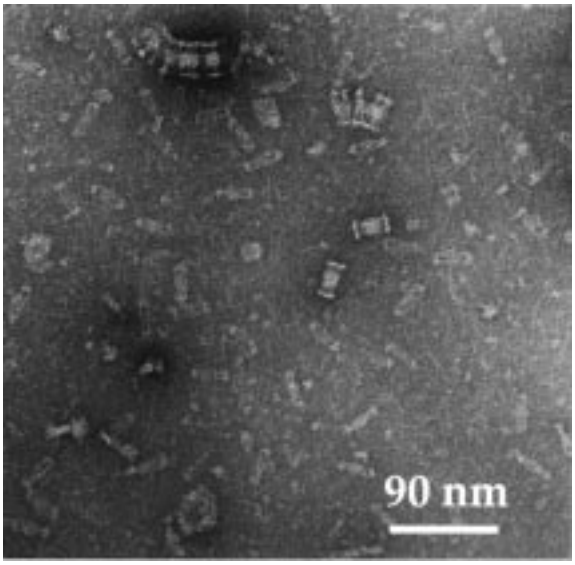

FIGURE 3: Electron micrograph of a negatively stained mixture of 45 μM LZ-Tar_c, 10 μM CheW, and 5.0 μM $CheA_{CR}$ after incubation at 30 °C for 4 h (Experimental Procedures).

The complexes were purified from incubation mixtures by molecular sieve chromatography (Figure 4). As with full-length CheA (*41*), more than 90% of the kinase activity eluted with the high molecular weight complex at approximately 15 min. To estimate the molecular weight of the complexes and their effective radii of gyration, an in-line light scattering detector was connected to the chromatography column. As expected, the elution time for the ternary complexes with $CheA_{CR}$ was slightly longer and the estimated molecular mass, 1.0 ± 0.3 MD, slightly smaller

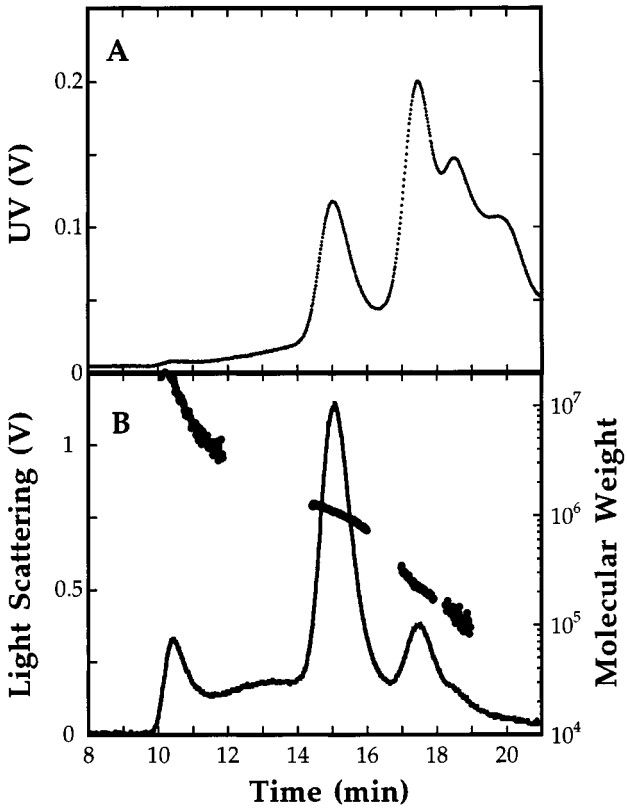

FIGURE 4: Molecular sieve chromatography and light scattering analysis of active complexes formed from all-Q LZ Tar_C, CheW, and $CheA_{CR}$. (A) A mixture containing 50 μM all-Q LZ-Tar_C, 10 μM CheW, and 10 μM $CheA_{CR}$ was incubated at 30 °C for 4 h and then subjected to molecular sieve chromatography with UV detection as described under Experimental Procedures. (B) Light scattering profile and computed molecular weights (indicated by a scan of values obtained at different points in the peak elution profiles) were generated from data collected by a miniDAWN detector as described under Experimental Procedures.

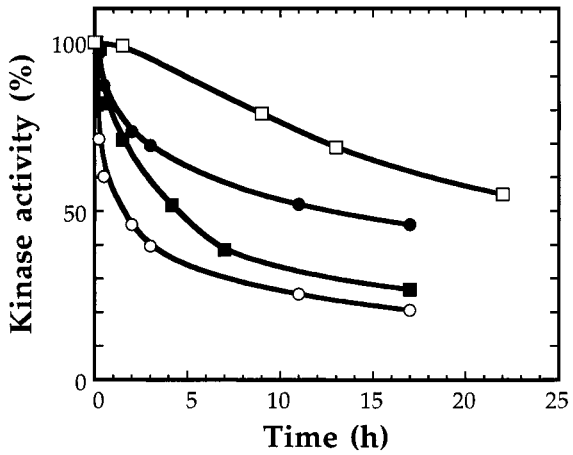

FIGURE 5: Effects of glutamyl modification and CheW on the stability of purified ternary complexes. Complexes formed from all-Q LZ-Tar_c or Q/E LZ-Tar_c were purified by molecular sieve chromatography as described under Experimental Procedures. Kinase activity was measured in the presence of 50 μM CheY and 2.0 mM ATP after incubation at room temperature for the indicated times. All-Q LZ-Tar_c (●), Q/E LZ-Tar_c(■), Q/E LZ-Tar_c plus 10 μM CheW (○). Data for all-Q LZ-Tar_c/CheW/CheA complexes (□) obtained using the same procedure (*41*) are shown for comparison. Results are presented as a percentage of the activity of complexes measured 5 min after elution from the column.

than that for the complexes with full-length CheA. The particles had a radius of gyration of approximately 20 nm (Figure 4B). The complexes formed from all-Q LZ-Tar_C were more stable than the complexes formed from Q/E LZ-Tar_C (Figure 5), the same as in the case of full-length CheA (*41*). Generally, the stability of the complexes with $CheA_{CR}$ is somewhat lower than with full-length CheA. Electron microscopic examination and molecular sieve chromatography showed that the loss of kinase activity was caused by dissociation of the ternary complexes. It has previously been observed with Tar receptor in membranes (*49, 50*) and LZ-Tar_C constructs (*9, 41*) that concentrations of CheW >10 μM dramatically reduce steady-state levels of ternary complex formation. High concentrations of CheA also exhibited inhibitory properties, but to a lesser extent (*41*). We have found that the same effects pertain with complexes formed by $CheA_{CR}$ (Figure 2). We have also found that, as with complexes formed from intact CheA, CheW stimulates the dissociation of isolated preformed complexes (Figure 5). All these results indicate that the complexes formed from $CheA_{CR}$ have essentially the same structure as those formed from full-length CheA (*41*).

Kinetics of CheA Histidine Kinase Activity in Ternary Complexes with All-Q LZ-Tar_C and CheW. CheA activity was determined using a coupled assay that measures the rate of hydrolysis of ATP by CheA in the presence of CheY under steady-state conditions where CheA autophosphorylation is limiting (i.e., no phospho-CheA can be detected, the rate does not depend on CheY concentration, and the rate varies linearly with the concentration of the ternary complex). Kinase activity at saturating concentrations of ATP and $CheA_H$ (in the case of the complexes with $CheA_{CR}$) was measured with complexes formed from all-Q LZ-Tar_C purified by molecular sieve chromatography. The activity of CheA was found to increase 96-fold upon incorporation into the ternary complexes (23 s^{-1} for CheA in complexes versus 0.24 s^{-1} for CheA alone), and the activity of $CheA_{CR}$ increases 63-fold (30 s^{-1} for $CheA_{CR}$ in complexes versus 0.48 s^{-1} for $CheA_{CR}$ alone) (Table 1). The dramatic activation of CheA kinase activity in ternary complexes formed from all-Q LZ-Tar_C and CheW is similar to the activation observed with complexes formed between CheA, CheW, and intact receptors in the membrane (*51*). We also determined the dependencies of the rate of the reaction on substrate concentration: ATP in the case of CheA, and both ATP and $CheA_H$ in the case of $CheA_{CR}$. The dependence of the rate of the reaction on [ATP] was hyperbolic. Incorporation into the ternary complexes resulted in an approximately 50% decrease in the apparent K_M for ATP both for CheA and for $CheA_{CR}$ at saturating concentrations of $CheA_H$ (Figure 6A,B, Table 1). The K_M values of ATP for CheA and $CheA_{CR}$ appear to be the same, indicating that the ATP-binding properties of the catalytic domain are unaffected by deletion of the N-terminal H- and YB-domains.

Table 1: Kinetic Constants for CheA and $CheA_{CR}$ Alone and in Complexes with All-Q LZ-Tar_C and CheW at Saturating Concentrations of the Substrates (see Legend to Figure 6)

	k_{obs} (s^{-1})	K_M for ATP (μM)	K_M for $CheA_H$ (μM)
CheA (alone)	0.24 ± 0.01	309 ± 4	–
CheA (complex)	23 ± 3	171 ± 9	–
$CheA_{CR}$ (alone)	0.48 ± 0.02	370 ± 16	26 ± 1
$CheA_{CR}$ (complex)	30 ± 10	181 ± 9	5.1 ± 0.3

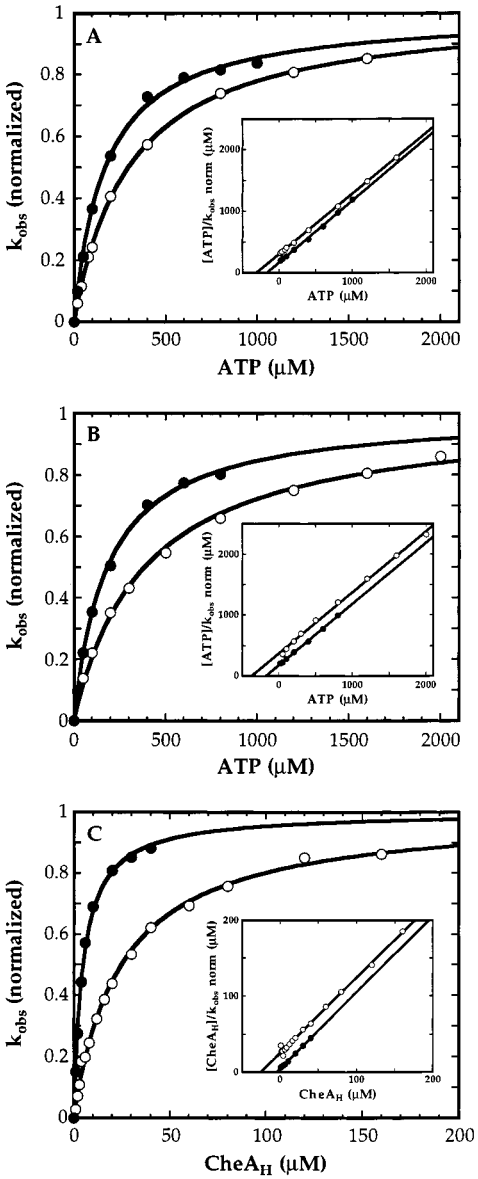

FIGURE 6: Effect of formation of ternary complexes with all-Q LZ-Tar$_c$ and CheW on the steady-state kinetic parameters of CheA and CheA$_{CR}$. The complexes were prepared and the rates of the reactions measured as described under Experimental Procedures. (A) Rates of CheA autophosphorylation in all-Q LZ-Tar$_c$−CheW−CheA complexes (●) and CheA alone (○) were measured as a function of ATP concentration. The concentration of the CheA subunits in the activity assay was 0.40 and 2.0 μM in the experiments with the complex and CheA alone, respectively. The inset shows the results plotted according to the method of Hanes (*52*). For plotting, the activities were normalized with respect to the values of k_{obs} at saturating substrate. Thus, in each figure, the slopes, corresponding to $1/k_{obs}$ at saturation, are identical. The curves represent the best fit of the experimental data to the Michaelis−Menten equation with parameters K_M for ATP of 171 ± 9 μM and k_{obs} of 23 ± 3 s^{-1} for the complex, and K_M for ATP of 309 ± 4 μM and k_{obs} of 0.24 ± 0.01 s^{-1} for CheA alone. (B and C) Rates of CheA$_H$ phosphorylation catalyzed by all-Q LZ-Tar$_c$−CheW−CheA$_{CR}$ complex (●) and CheA$_{CR}$ alone (○) were measured as a function of ATP (B) or CheA$_H$ (C) concentrations in the presence of 100 μM CheA$_H$ (B) or 2000 μM ATP (C). The kinetic parameters determined at other concentrations of CheA$_H$ and ATP are shown in Table 2. The curves represent the best fit of the experimental data to the Michaelis−Menten equation with parameters K_M for CheA$_H$ of 5.1 ± 0.3 μM, K_M for ATP of 181 ± 9 μM, and k_{obs} of 30 ± 10 s^{-1} for all-Q LZ-Tar$_c$−CheW−CheA$_{CR}$ complex; and K_M for CheA$_H$ of 26 ± 1 μM, K_M for ATP of 370 ± 16 μM, and k_{obs} of 0.48 ± 0.02 s^{-1} for CheA$_{CR}$ alone.

Table 2: Effect of ATP or CheA$_H$ Concentration on K_M Values for the LZ-Tar$_C$−CheW−CheA$_{CR}$ Complexes (see Legend to Figure 6)[a]

	CheA$_H$ (μM)		
	2.5	10	100
K_M for ATP (μM)	313 ± 40 (307)	194 ± 10 (243)	181 ± 9 (189)
	ATP (μM)		
	40	100	2000
K_M for CheA$_H$ (μM)	8.1 ± 0.7 (9.3)	7.1 ± 0.5 (8.3)	5.1 ± 0.3 (5.4)

[a] The values of the K_M's predicted using the expressions for the K_M's shown in the legend to Figure 7 and kinetic parameters from Table 3 are shown in parentheses (see Results for explanations).

The dependence of the rate of CheA$_H$ phosphorylation by CheA$_{CR}$ as a function of CheA$_H$ concentration also was hyperbolic. The results (Figure 6C, Table 1) show a decrease in K_M, from 26 μM for CheA$_{CR}$ alone to 5.1 μM for CheA$_{CR}$ in active ternary complexes at saturating concentrations of ATP.

To look for possible cooperative interactions between CheA$_H$ and ATP, we have measured the dependence of the K_M values for ATP on CheA$_H$ concentration and vice versa (Table 2). The results indicate that in the ternary complexes the apparent K_M's for both ATP and CheA$_H$ decrease when the concentration of the second substrate increases. This apparent cooperativity in substrate binding was not observed, however, for free CheA$_{CR}$. The same lack of dependence was observed in a previous study of CheA$_H$ phosphorylation by the isolated catalytic domain of CheA, CheA$_C$ (*29*).

Kinetic Model for CheA Regulation. We propose the following model to describe the steady-state reactions of H-domain phosphorylation by ATP catalyzed by the C-domain of CheA (Figure 7).

(i) We postulate that the kinase can exist in two distinct states with respect to H-domain binding to the catalytic site: an inactive conformation (C), wherein the H-domain is loosely associated and phosphotransfer cannot occur; and an active conformation (C*), wherein the H-domain is tightly bound (buried) and cannot dissociate and the phosphoaccepting histidine is properly positioned for subsequent phosphotransfer. This postulate is based on the following logic. Considering a simple enzymatic reaction:

$$E + S \underset{k_{-1}}{\overset{k_1}{\rightleftarrows}} E{\cdot}S \xrightarrow{k_{cat}} E + P$$

where $K_M = (k_{-1} + k_{cat})/k_1$, one can see that an increase in the reaction rate constant k_{cat} will result, on one hand, in an increase of the rate of the reaction, but, on the other hand, it will, if anything, result in an increase rather than a decrease in the K_M. Since we observed *both* an increase in V_{max} and a decrease in K_M, we postulate the presence of an equilibrium between inactive and active enzyme−substrate complexes. A shift in this equilibrium can then explain the simultaneous increase in the V_{max} and the decrease in the K_M for the substrates, CheA$_H$ and ATP, associated with CheA activation.

(ii) The structure of the transition state of the enzyme−substrate complex, i.e., the molecular mechanism of catalysis, is assumed to be the same for CheA alone and for CheA in complexes with receptor and CheW. CheA activation within the ternary complexes is seen to result from a shift in the

equilibrium between the inactive and active states, i.e., a decrease of K*, while the rate of phosphotransfer itself (k_{cat}) as well as the dissociation constants (K_{ATP} and K_H) remain unchanged.

(iii) Based on the similarities of structural and kinetic properties of CheA and $CheA_{CR}$, we assume that the H-domain, when it is a part of the full-length CheA protein, functions similarly to the free protein, $CheA_H$.

(iv) We assume that the kinase reaction obeys a random-order of binding mechanism typical for phosphotransferase enzymes (*52*), where binding of one substrate does not directly affect binding of another substrate. This means that the dissociation constants for the complex of the catalytic domain with one substrate (C·ATP and C·H) are the same as for the complex with two substrates (C·ATP·H). According to the model, an activated complex can form in the absence of ATP (C*·H), thus introducing asymmetry into the reaction pathway. The effect of ATP binding on the activation as well as the effect of the activation on ATP binding is reflected by the coefficient *r*.

(v) All substrate binding steps and interconversions between inactive and active forms of the enzyme−substrate complexes are assumed to be at equilibrium, with the rate-limiting step of the reaction being phosphotransfer. This assumption, which greatly simplifies the kinetic analysis, seems reasonable because of the low ($<30\ s^{-1}$) rate of the reaction.

(vi) The phosphotransfer step is shown as an irreversible reaction. The kinetic measurements were performed under conditions to ensure that this assumption holds, with an excess of CheY to prevent accumulation of the phosphorylated H-domain, and the presence of phosphoenolpyruvate (PEP) and pyruvate kinase (PK) to efficiently convert the ADP formed in the reaction back to ATP.

Quantitative Evaluation of the Kinetic Model. The kinetic scheme can be described by a system of equilibrium equations and the mass balance equation:

$$[C^*\cdot H] = (rK_{ATP}/[ATP])[C^*\cdot ATP\cdot H]$$

$$[H\cdot C\cdot ATP] = K^*[C^*\cdot ATP\cdot H]$$

$$[H\cdot C] = (K_{ATP}/[ATP])[H\cdot C\cdot ATP]$$

$$[C\cdot ATP] = (K_H/[H])[H\cdot C\cdot ATP]$$

$$[C] = (K_{ATP}/[ATP])[C\cdot ATP]$$

$$[C]_{total} = [C] + [C\cdot ATP] + [H\cdot C] + [H\cdot C\cdot ATP] + [C^*\cdot H] + [C^*\cdot ATP\cdot H]$$

Solving this system for [C*·ATP·H], we can obtain an expression for the observed rate constant, k_{obs}, which is proportional to the concentration of the active form of the enzyme−substrate complex:

$$k_{obs} = k_{cat}\frac{[C^*\cdot ATP\cdot H]}{[C]_{total}} = k_{cat}\frac{1}{(K_{ATP}/[ATP] + 1)(K^*(K_H/[H] + 1) + r) + 1 - r}$$

From this we can find the expressions for K_M for ATP and the H-domain, K_M^{ATP} and K_M^H, i.e., the substrate concentrations at which the reaction rate is half the maximal value achieved when the concentration of the substrate is saturating and the concentration of the second substrate is constant:

$$K_M^{ATP} = \left(1 + \frac{r - 1}{K^*(K_H/[H] + 1) + 1}\right)K_{ATP}$$

$$K_M^{H} = \frac{K^*}{K^* + r + (1 - r)/(K_{ATP}/[ATP] + 1)}K_H$$

These expressions can be simplified for a situation when one or both substrates are at saturating concentrations:

$$k_{obs} = \frac{k_{cat}}{K^* + 1} \quad \text{at saturating [ATP] and [H]}$$

$$K_M^{ATP} = \frac{K^* + r}{K^* + 1}K_{ATP} \quad \text{at saturating [H]}$$

$$K_M^{H} = \frac{K^*}{K^* + 1}K_H \quad \text{at saturating [ATP]}$$

The values of k_{obs}, K_M^{ATP}, and K_M^H at these conditions were estimated both for $CheA_{CR}$ alone and for $CheA_{CR}$ in the ternary complexes (Table 1). Thus, we can write a system of six equations (three for each of the forms) with six unknowns: k_{cat}, *r*, K_{ATP}, and K_H (common for $CheA_{CR}$ alone and for $CheA_{CR}$ in the ternary complexes); and K^* and $K^{*\prime}$ for $CheA_{CR}$ alone and for $CheA_{CR}$ in the ternary complexes, respectively. Solving this system analytically, we can obtain the values of these kinetic parameters (Table 3).

One can show by analyzing the expressions for K_M's that their values are expected to increase when the concentration of the other substrate decreases. K_M^H is expected to change its value from $K_HK^*/(K^* + r)$, when [ATP] → 0, to $K_HK^*/(K^* + 1)$, when [ATP] → ∞. K_M^{ATP} is expected to change from K_{ATP}, when [H] → 0, to $K_{ATP}(K^* + r)/(K^* + 1)$, when [H] → ∞. When $K^* \gg 1$, as in the case of $CheA_{CR}$ alone, these changes are negligible, as was observed, and the values of K_M^{ATP} and K_M^H are equal to the values of the corresponding binding constants, K_{ATP} and K_H. In the case of $CheA_{CR}$

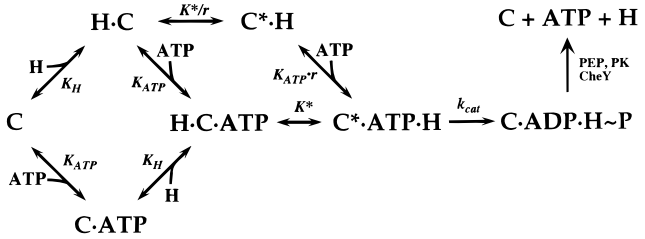

FIGURE 7: Kinetic model for CheA autophosphorylation (H-domain phosphorylation). C and H correspond to the C- and H-domains of CheA; K_{ATP} and K_H are dissociation constants of the C·ATP and H·C complexes; K^* is an equilibrium constant for the interconversion between the inactive form of the enzyme−substrate complex, H·C·ATP, and its activated form, C*·ATP·H; the coefficient *r* reflects the effect of activation on ATP binding, and k_{cat} is the rate constant of phosphotransfer within the active complex. PK and PEP correspond to pyruvate kinase and phosphoenolpyruvate.

Table 3: Values for the Kinetic Constants Describing the Scheme in Figure 7

constant	K_H (μM)	K_{ATP} (μM)	*r*	k_{cat} (s^{-1})	K^*	$K^{*\prime}$
value	26	370	0.36	37	77	0.24

in the ternary complexes, when $K^* < 1$, the changes are expected to be much more pronounced. Thus, the apparent synergism in the substrate binding results rather from the increased conversion of the ternary complex into its active state, than from the direct cooperative effect of the binding of one substrate on the binding of another substrate. To check out how well our experimental data satisfy the model, we put the kinetic parameters calculated using the data obtained at saturating concentrations of the substrates (Table 3) into the equations for the K_M's to calculate the values of the K_M's expected at subsaturating concentrations of the second substrate. The predicted values for the K_M's are shown in Table 2 in parentheses. The fit of the predicted values to those determined experimentally is entirely consistent with the proposed kinetic model.

DISCUSSION

We have previously characterized the formation and structure of the soluble active complexes formed between a Tar receptor construct containing its cytoplasmic part fused to a leucine zipper (LZ-Tar_C), CheW, and CheA (*41*). Here we present a detailed kinetic analysis of these complexes. To investigate the effect of activation on domain interactions within CheA, we have engineered two CheA constructs: $CheA_H$, corresponding to the phosphoaccepting H-domain; and $CheA_{CR}$, corresponding to the catalytic (C) and regulatory (R) domains. The complexes formed by LZ-Tar_C, CheW, and $CheA_{CR}$ appear to be essentially the same as those formed from full-length CheA. HPLC, light scattering, and electron microscopic studies revealed the same well-defined structures that we have previously observed with full-length CheA (*41*). The kinetic properties of CheA and $CheA_{CR}$ in the ternary complexes (k_{obs}, K_M for ATP) are also similar. This supports the view that the H-domain functions as an essentially independent phosphoaccepting domain within the intact CheA protein, and that receptor activation does not require the YB-domain of CheA that binds the chemotaxis response regulator, CheY. This result is consistent with the observation that gene fragments encoding $CheA_H$ are able to support chemotactic signaling by H-domain-deficient CheA mutants (*53*).

No values have been reported for the V_{max} of CheA autophosphorylation in ternary complexes formed with intact receptors in membranes. Typically, the amounts of phospho-CheY generated by CheA alone and CheA in the complexes over a specified time interval have been compared to obtain estimates of the degree of CheA activation (*49, 51*). By these criteria, the level of activation depends both on CheA activity within the complex, which is generally measured at conditions optimized for complex formation, and on the activity of pure CheA under the same conditions, which are generally far from optimal. For example, in the most often quoted experiments, the degree of CheA activation in complexes was estimated to be about 300-fold (*51*) under conditions where the rate for CheA alone was measured at a concentration of 0.25 μM when approximately half of the kinase would be expected to be present as inactive monomers (*26*). The 100-fold increase of CheA activity that we observe with ternary complex formed from soluble LZ-Tar_c is therefore essentially equivalent to that seen in membranes.

We have proposed a model to describe the kinetic phenomena accompanying activation of CheA in the ternary complexes—a dramatic increase of the rate of autophosphorylation with a corresponding decrease in the K_M's for both ATP and the H-domain. We have postulated that there is an equilibrium between two forms of substrate−kinase complexes: an inactive complex where the phosphoaccepting H-domain is loosely bound, and an activated form, where the phosphoaccepting domain is tightly associated with the kinase active site and properly positioned for phosphotransfer (Figure 8). According to this model, the rate of the reaction is a function of the equilibrium between active and inactive forms, which is allosterically regulated by associated receptors.

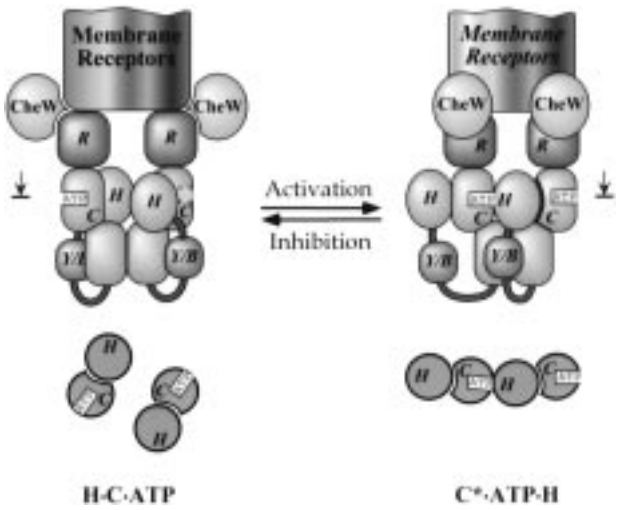

FIGURE 8: A model for the mechanism of CheA regulation in receptor signaling complexes (side view and top view at the imaginary cross section indicated by arrows).

Earlier we proposed a mechanism of asymmetric activation of CheA by receptors where only one phosphoaccepting H-domain at a time can interact with an active site within a CheA dimer (*29*). Recent ATP-binding studies also indicate that although there are two ATP-binding sites per CheA dimer, only one of them at a time appears to participate in catalysis (*36*). Kinase activation could follow from a conformational change in the receptor−kinase complex that favors formation of an asymmetric relationship between the phosphoaccepting H-domain and the ATP-binding catalytic C-domain, which in kinetic terms means a shift of the equilibrium toward the activated form of the enzyme (C*·ATP·H) wherein the H-domain is properly positioned for phosphotransfer. On the other hand, inhibition could result from receptor inputs that preclude formation of this form of the enzyme.

At least two considerations support the idea that CheA undergoes large-amplitude motions during autophosphorylation. First, the catalytic domain must bind the H-domain, phosphorylate it, and then release it for subsequent phosphotransfer to the response regulators CheY or CheB. Second, the ATP-binding C-domain of histidine kinases has recently been shown to be homologous to the type II topoisomerase GyrB and protein chaperone Hsp90 (*54*), and in both these proteins ATP binding and phosphotransfer are coupled to substantial molecular movements.

ACKNOWLEDGMENT

We thank Michael Surette for providing the $CheA_{CR}$ overproducing strain, Tatiana Tolstykh for providing purified

proteins, and Thorsten Grebe for useful comments on the manuscript.

REFERENCES

1. Stock, J. B., and Surette, M. (1996) in *Escherichia coli and Salmonella typhimurium*: *Cellular and Molecular Biology* (Neidhardt, F. C., Ed.) pp 1103−1129, ASM, Washington, D.C.
2. Falke, J. J., Bass, R. B., Butler, S. L., Chervitz, S. A., and Danielson, M. A. (1997) *Annu. Rev. Cell. Dev. Biol. 13*, 457−512.
3. Manson, M. D., Armitage, J. P., Hoch, J. A., and Macnab, R. M. (1998) *J. Bacteriol. 180*, 1009−1022.
4. Goudreau, P. N., and Stock, A. M. (1998) *Curr. Opin. Microbiol. 1*, 160−169.
5. Levit, M. N., Liu, Y., and Stock, J. B. (1998) *Mol. Microbiol. 30*, 459−466.
6. Scott, W. G., Milligan, D. L., Milburn, M. V., Prive, G. G., Yeh, J., Koshland, D. E., Jr., and Kim, S. H. (1993) *J. Mol. Biol. 232*, 555−573.
7. Yeh, J. I., Biemann, H. P., Prive, G. G., Pandit, J., Koshland, D. E., Jr., and Kim, S. H. (1996) *J. Mol. Biol. 262*, 186−201.
8. Chi, Y. I., Yokota, H., and Kim, S. H. (1997) *FEBS Lett. 414*, 327−332.
9. Surette, M. G., and Stock, J. B. (1996) *J. Biol. Chem. 271*, 17966−17973.
10. Seeley, S. K., Wittrock, G. K., Thompson, L. K., and Weis, R. M. (1996) *Biochemistry 35*, 16336−16345.
11. Seeley, S. K., Weis, R. M., and Thompson, L. K. (1996) *Biochemistry 35*, 5199−5206.
12. Le Moual, H., and Koshland, D. E., Jr. (1996) *J. Mol. Biol. 261*, 568−585.
13. Bass, R. B., and Falke, J. J. (1998) *J. Biol. Chem. 273*, 25006−25014.
14. Danielson, M. A., Bass, R. B., and Falke, J. J. (1997) *J. Biol. Chem. 272*, 32878−32888.
15. Liu, J. D., and Parkinson, J. S. (1991) *J. Bacteriol. 173*, 4941−4951.
16. Lupas, A., Van Dyke, M., and Stock, J. (1991) *Science 252*, 1162−1164.
17. Stock, J. B., Lukat, G. S., and Stock, A. M. (1991) *Annu. Rev. Biophys. Biophys. Chem. 20*, 109−136.
18. Cochran, A. G., and Kim, P. S. (1996) *Science 271*, 1113−1116.
19. Djordjevic, S., and Stock, A. M. (1997) *Structure 5*, 545−558.
20. Djordjevic, S., and Stock, A. M. (1998) *Nat. Struct. Biol. 5*, 446−450.
21. West, A. H., Martinez-Hackert, E., and Stock, A. M. (1995) *J. Mol. Biol. 250*, 276−290.
22. Anand, G. S., Goudreau, P. N., and Stock, A. M. (1998) *Biochemistry 37*, 14038−14047.
23. Djordjevic, S., Goudreau, P. N., Xu, Q., Stock, A. M., and West, A. H. (1998) *Proc. Natl. Acad. Sci. U.S.A. 95*, 1381−1386.
24. Milligan, D. L., and Koshland, D. E., Jr. (1988) *J. Biol. Chem. 263*, 6268−6275.
25. Milligan, D. L., and Koshland, D. E., Jr. (1993) *J. Biol. Chem. 268*, 19991−19997.
26. Surette, M. G., Levit, M., Liu, Y., Lukat, G., Ninfa, E. G., Ninfa, A., and Stock, J. B. (1996) *J. Biol. Chem. 271*, 939−945.
27. Parkinson, J. S., and Kofoid, E. C. (1992) *Annu. Rev. Genet. 26*, 71−112.
28. Swanson, R. V., Schuster, S. C., and Simon, M. I. (1993) *Biochemistry 32*, 7623−7629.
29. Levit, M., Liu, Y., Surette, M., and Stock, J. (1996) *J. Biol. Chem. 271*, 32057−32063.
30. Zhou, H., Lowry, D. F., Swanson, R. V., Simon, M. I., and Dahlquist, F. W. (1995) *Biochemistry 34*, 13858−13870.
31. Zhou, H., and Dahlquist, F. W. (1997) *Biochemistry 36*, 699−710.
32. Li, J., Swanson, R. V., Simon, M. I., and Weis, R. M. (1995) *Biochemistry 34*, 14626−14636.
33. McEvoy, M. M., Hausrath, A. C., Randolph, G. B., Remington, S. J., and Dahlquist, F. W. (1998) *Proc. Natl. Acad. Sci. U.S.A. 95*, 7333−7338.
34. Welch, M., Chinardet, N., Mourey, L., Birck, C., and Samama, J. P. (1998) *Nat. Struct. Biol. 5*, 25−29.
35. Stock, J. B., Surette, M. G., Levit, M., and Park, P. (1995) in *Two-Component Signal Transduction* (Hoch, J. A., and Silhavy, T. J., Eds.) pp 25−51, ASM, Washington, D.C.
36. Stewart, R. C., VanBruggen, R., Ellefson, D. D., and Wolfe, A. J. (1998) *Biochemistry 37*, 12269−12279.
37. Morrison, T. B., and Parkinson, J. S. (1994) *Proc. Natl. Acad. Sci. U.S.A. 91*, 5485−5489.
38. Zhou, H., McEvoy, M. M., Lowry, D. F., Swanson, R. V., Simon, M. I., and Dahlquist, F. W. (1996) *Biochemistry 35*, 433−443.
39. Tawa, P., and Stewart, R. C. (1994) *Biochemistry 33*, 7917−7924.
40. Stewart, R. C. (1997) *Biochemistry 36*, 2030−2040.
41. Liu, Y., Levit, M., Lurz, R., Surette, M., and Stock, J. (1997) *EMBO J. 16*, 7231−7240.
42. Maddock, J. R., and Shapiro, L. (1993) *Science 259*, 1717−1723.
43. Stock, A., Mottonen, J., Chen, T., and Stock, J. (1987) *J. Biol. Chem. 262*, 535−537.
44. Stock, A., Chen, T., Welsh, D., and Stock, J. (1988) *Proc. Natl. Acad. Sci. U.S.A. 85*, 1403−1407.
45. Stock, A., Koshland, D. E., Jr., and Stock, J. (1985) *Proc. Natl. Acad. Sci. U.S.A. 82*, 7989−7993.
46. Wyatt, P. J. (1993) *Anal. Chim. Acta 272*, 1−40.
47. Wen, J., Arakawa, T., and Philo, J. S. (1996) *Anal. Biochem. 240*, 155−166.
48. Gill, S. C., and von Hippel, P. H. (1989) *Anal. Biochem. 182*, 319−326.
49. Ninfa, E. G., Stock, A., Mowbray, S., and Stock, J. (1991) *J. Biol. Chem. 266*, 9764−9770.
50. Gegner, J. A., Graham, D. R., Roth, A. F., and Dahlquist, F. W. (1992) *Cell 70*, 975−982.
51. Borkovich, K. A., Kaplan, N., Hess, J. F., and Simon, M. I. (1989) *Proc. Natl. Acad. Sci. U.S.A. 86*, 1208−1212.
52. Dixon, M., and Webb, E. C. (1979) *Enzymes*, Academic Press Inc., New York.
53. Garzon, A., and Parkinson, J. S. (1996) *J. Bacteriol. 178*, 6752−6758.
54. Tanaka, T., Saha, S. K., Tomomori, C., Ishima, R., Liu, D., Tong, K. I., Park, H., Dutta, R., Qin, L., Swindells, M. B., Yamazaki, T., Ono, A. M., Kainosho, M., Inouye, M., and Ikura, M. (1998) *Nature 396*, 88−92.

BI982839L